# Surface-Directed and Ethanol-Induced DNA Condensation on Mica

**Ce Zhang and Johan R. C. van der Maarel***

*National University of Singapore, Department of Physics, 2 Science Drive 3, Singapore 117542*

*Received: September 24, 2007; In Final Form: January 1, 2008*

The adsorption of $\lambda$-phage DNA onto mica was investigated with atomic force microscopy. We found that the morphologies depended on the solvent conditions in the sample preparation procedure. Flat-lying networks of hybridized single-stranded DNA were obtained if ultrapure water was used. If buffered conditions are maintained during the whole of the preparation procedure, single double-stranded DNA molecules are adsorbed. The adsorbed double-stranded DNA molecules subsequently can be condensed in situ on the surface by a brief rinse with anhydrous ethanol in the presence of divalent magnesium cations. The majority of these surface-directed and ethanol-induced condensed structures are toroids, but a small fraction of rods also has been observed. Analysis of the height and lateral dimensions shows that the toroids are single-molecular and disk-like with a height of one to two DNA diameters. The thin toroid morphology appears to be a general phenomenon of surface-directed condensation, irrespective of the nature of the condensing ligands and the specific surface interaction.

## Introduction

In biological systems such as cells and viruses, DNA is found in tightly packaged states. The structural organization within these states is largely unknown but bears some resemblance to condensed DNA phases observed in vitro. The term condensed refers to situations in which the DNA assembly has an orderly morphology, in contrast to precipitates or aggregates with a disordered molecular arrangement. Model systems that can produce condensed DNA phases are hence of great interest for understanding the mechanisms involved in vivo. DNA condensation can be induced by the addition of condensing agents and/or ligands (e.g., multivalent cations of valence three or greater, cationic polypeptides such as polylysine, basic proteins, alcohols, and neutral crowding polymers).[1] When condensation is induced by the addition of a condensing agent to very dilute DNA solutions at low ionic strength, toroids and rods are observed.[2] At higher DNA concentrations, liquid crystals are formed.[3,4]

DNA condensation also can be assisted and directed by a surface. Surface-directed condensation is particularly relevant from a biophysical point of view because the interface can be considered to be a model system for the scaffolding inside the cell. In surface-directed condensation, DNA is first adsorbed onto a surface, after which it is condensed with a condensing agent. Examples that have been reported in the literature are the condensation of single DNA molecules with basic protein nucleoprotamine and silanes.[5,6] In the former case, DNA was first loosely bound to a mica surface with the help of $MgCl_2$, after which well-defined toroidal structures were formed by the subsequent addition of the nucleoprotamine. Silanes are functionalized cationic polyamines that loosely bind to a silicon surface. The surface adsorbed silanes are hence mobile and were observed to bind and condense DNA in rods and toroids. As in the solution studies, DNA is condensed by cationic agents, but the surface-directed toroidal structures are rather spread out and thin with a height on the order of one to two DNA diameters (2−4 nm).

Condensed DNA structures adsorbed onto a surface also can be obtained by dropping a droplet of a highly diluted DNA solution onto a mica surface, transferring the specimen to ultrapure water for development, followed by a rinse with anhydrous ethanol.[7,8] This procedure results in flat-lying and densely packed DNA network structures. During the development process, these structures are supposedly produced by contacting, crossing, and overlapping DNA chains, as well as by hybridizing complementary bases of sticky ends created by sample handling (see ref 8 and references therein). The final rinse with anhydrous ethanol stops the development process and enhances the stabilization of the DNA film. Since ethanol is also known to condense highly diluted DNA into single-molecular rod and toroidal structures,[9,10] the formation of the flat-lying DNA networks seems to be at odds with the previously mentioned surface-assisted condensation experiments.[5,6]

In the present study, we systematically explored the conditions under which single-molecular or extended network structures of bacteria $\lambda$-phage DNA (48 502 base pairs, contour length in the *B*-form of 16.5 $\mu$m) on mica can be obtained. We showed that the morphologies critically depend on the solvent and buffer conditions in the preparation procedure. We also showed that single $\lambda$-phage DNA molecules can be condensed by a rinse of the specimen with anhydrous ethanol after the molecules have been adsorbed onto the mica with divalent magnesium cations. Finally, the condensed nanostructures resulting from this surface-directed and ethanol-induced condensation process were analyzed and characterized with atomic force microscopy (AFM).

## Experimental Procedures

Bacteria $\lambda$-phage DNA was purchased from New England Biolabs, Ipswich, MA and used without further purification. As received from the manufacturer, the $\lambda$-phage DNA stock solution had a concentration of 0.5 g of DNA/L. The solvent is TE buffer, which is composed of 10 mM Tris-HCl, pH 8.0, and 1 mM EDTA. Anhydrous ethanol was purchased from SINO,

* Corresponding author. Tel.: 65 65164396; fax: 65 67776126; e-mail: phyjrcvd@nus.edu.sg.

10.1021/jp0776560 CCC: $40.75 © 2008 American Chemical Society
Published on Web 02/23/2008

Singapore. Water was deionized and purified by a Millipore system and had a conductivity less than $1 \times 10^{-6}$ $\Omega^{-1}$ $cm^{-1}$. Muscovite mica was purchased from Structure Probe, West Chester, PA and cut into approximately 1 $cm^2$ square pieces. Both sides of the mica surface were always freshly cleaved before use.

For adsorption studies, the stock solution was diluted 100 times to a final $\lambda$-phage DNA concentration of 5 mg/L. For this initial dilution step, we used TE buffer (method A) or ultrapure water (method B). The 100-fold diluted stock was then mixed with a 2 mM $MgCl_2$ solution in a 1:1 volume ratio and incubated at 38 °C for 1 h. A 20 $\mu$L droplet (2.5 mg/L DNA and 1 mM $MgCl_2$) was spotted onto a fleshly cleaved mica surface. After 8 min to allow for DNA adsorption onto the mica surface, the specimens were developed by immersing them in TE buffer (method A) or ultrapure water (method B) for 30 min. Following development, most specimens were rinsed with anhydrous ethanol for approximately 3 s and subsequently dried under ambient conditions.

All imaging experiments were carried out at room temperature in air with a Dimension 3000 atomic force microscope, Veeco, Woodbury, NY. Images were acquired in the tapping mode with silicon (Si) cantilevers (spring constant of 20−100 N/m) and operated below their resonance frequency (typically 230−410 kHz). The images were flattened, and the contrast and brightness were adjusted for optimum viewing conditions. The inner diameter, outer diameter, and height of the toroidal structures were always measured in nine different directions away from the center of the toroid with an angular increment of 40° with the NanoScope software. The estimated experimental resolution in height was 0.2 nm, but in the lateral direction, the 5 nm resolution was worse due to the finite sharpness of the atomic force microscope tip.

## Results and Discussion

**Effect of Dilution Conditions.** DNA is often dispersed in a buffer medium such as TE with an ionic strength in the millimolar range. In AFM adsorption studies, it is necessary to spot a highly diluted solution with a concentration in the range of 1−10 mg of DNA per liter on a flat surface such as mica. Since DNA is usually available at much higher concentrations, spotting solutions need to be prepared by dilution with the appropriate medium. In recent works, the stock solution was diluted up to 200-fold with ultrapure water to a final concentration of 2.5 mg of DNA/L, then mixed and incubated with a magnesium salt solution, and subsequently spotted onto a surface for adsorption, followed by development in pure water for various times.[7,8] This procedure resulted in flat-lying and densely packed DNA network structures. Since the double-helical structure of DNA is known to be unstable without a supportive electrolyte, we suspect that the surface-directed DNA network morphologies are related to the high dilution in ultrapure water and concomitant (partial) melting of the double helix.

To verify the effect of the dilution conditions on the surface morphologies, we prepared specimens by dilution and development with TE buffer (method A) as well as with ultrapure water (method B). After the initial dilution step, the DNA solutions were mixed and incubated with $MgCl_2$ solution at a slightly elevated temperature for 1 h. Solution droplets (2.5 mg/L DNA and 1 mM $MgCl_2$) were then spotted on freshly cleaved mica and developed in TE buffer (method A) or ultrapure water (method B) for 30 min. Since mica carries a negative surface charge, the $Mg^{2+}$ ions serve as a bridge and allow DNA molecules to adsorb. During development, excess $MgCl_2$ is diluted away from the interface, and the DNA molecules rearrange themselves and form a specific surface-directed morphology depending on the preparation procedure (i.e., method A vs method B). The specimens were air-dried but not rinsed with anhydrous ethanol. Representative tapping mode AFM images are displayed in Figure 1. If method A is followed, individual $\lambda$-phage DNA molecules are clearly discernible. Owing to the high magnification of the AFM instrument, only sections of the molecule are visible. The DNA molecules were extended and stretched out on the surface, probably related to surface tension effects during the air-drying process. The measured height of these adsorbed DNA molecules was 1.5 ± 0.3 nm. In the case of dilution and development in ultrapure water (method B), the AFM images were fundamentally different. In the latter case, DNA networks were observed. The height of the connecting DNA sections of these networks was only 0.3 ± 0.1 nm.

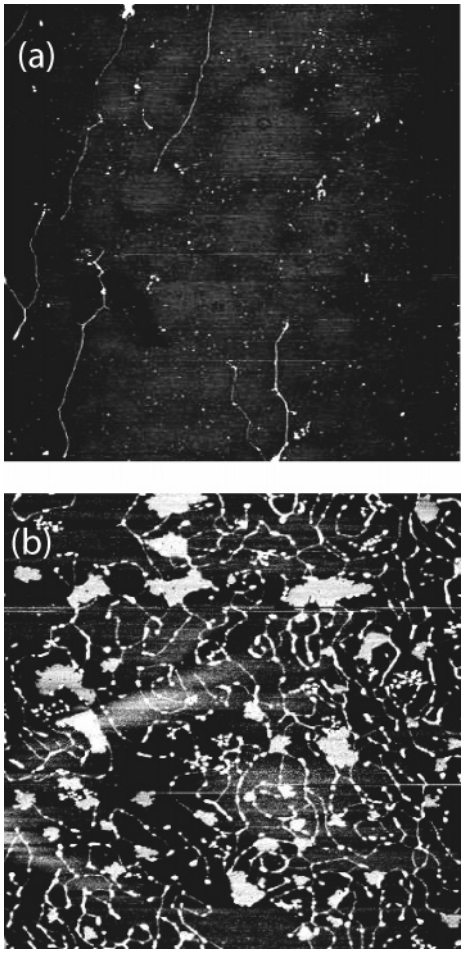


**Figure 1.** Typical tapping mode AFM images of $\lambda$-phage DNA (2.5 mg/L DNA, 1 mM $MgCl_2$) on mica. The images represent a 3.3 $\mu$m × 3.3 $\mu$m area. For initial dilution and sample development, TE buffer (method A, panel a) or ultrapure water (method B, panel b) was used. The specimens were air-dried but not washed with ethanol.

Double-stranded DNA is known to be unstable in the absence of supporting electrolytes due to the unscreened electrostatic repulsion of the phosphate moieties of the opposing strands in the double helix. Accordingly, we suspect that the double helix (partially) melts in the 100-fold dilution step with ultrapure water (method B) before it is mixed and incubated with the $MgCl_2$ solution. At the mica surface, the single-stranded DNA segments can then hybridize with other segments and thus form a densely packed and flat-lying network. This also explains the relatively small value of the height of the segments of this network, which

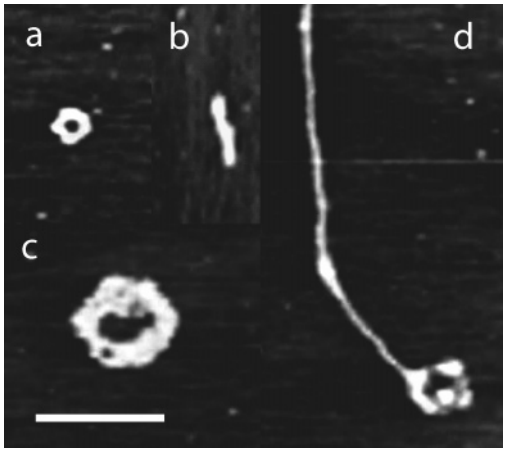


**Figure 2.** Composition tapping mode AFM images of condensed $\lambda$-phage DNA structures. A 2.5 mg/L DNA, 1 mM $MgCl_2$ solution was prepared according to method A, spotted onto a freshly cleaved mica surface, and developed for 30 min in TE buffer followed by a rinse with anhydrous ethanol. Toroidal structures are displayed in panels a and c, whereas panel b represents a typical rod structure. A partially condensed toroidal structure is displayed in panel d. The scale bar represents 0.5 $\mu$m.

is the same as the value reported for single-stranded DNA adsorbed on 3-aminopropyl triethoxysilane (APTES) modified mica ($0.3 \pm 0.1$ nm).[11] If the ionic strength is maintained at a sufficiently high level to stabilize the double-helical structure during the whole of the preparation procedure (TE buffer conditions), the images clearly show sections of individual $\lambda$-phage DNA molecules with a height $1.5 \pm 0.3$ nm. Because of compression effects by the AFM tip and/or the fact that the specimens are air-dried, the measured height is somewhat smaller than the outer diameter of the duplex in the *B*-form (2 nm).[12−14]

**Ethanol-Induced Condensation.** Under TE buffer conditions, $\lambda$-phage DNA molecules can be adsorbed onto mica with the help of divalent magnesium ions (method A). The tapping mode AFM images revealed extended molecules with a height measured from the surface in agreement with the value expected for the Watson−Crick double helix in the *B*-form. We showed that these adsorbed molecules can be condensed in situ on the mica surface by a brief wash of the specimens in anhydrous ethanol. As displayed in Figure 2, the condensed structures take the form of toroids, rods, and partially condensed toroids with a single protruding linear segment. Furthermore, DNA aggregation and/or network formation was not observed, although some of the toroids may contain multiple $\lambda$-phage DNA molecules.

Our procedure differs from previously reported work on ethanol-induced DNA condensation. The common procedure is to incubate a DNA solution with ethanol in the presence of soluble multivalent cations of valence three or greater such as spermidine or cobalt hexamine prior to the adsorption on a surface.[1,9] Fang et al. have shown that ethanol can induce DNA condensation in the presence of divalent magnesium only, but, again, a DNA solution was incubated with ethanol, and the condensed structures were formed in the bulk phase and not surface-directed.[10] We obtained the condensed structures by a scaffolding-assisted and ethanol-induced condensation of single DNA molecules adsorbed onto the mica surface with magnesium cations. Note that the magnesium cations serve to attach the DNA molecules to the surface and that they also can induce condensation, provided the dielectric constant of the medium is reduced by the addition of alcohol.[1,15]

An important feature of ethanol is that it also can induce a transition in the secondary structure of double-stranded DNA

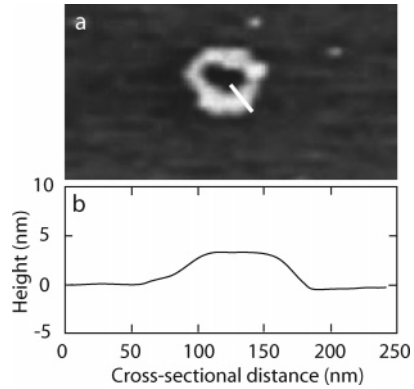


**Figure 3.** (a) Tapping mode AFM image of surface-directed and ethanol-induced toroid of $\lambda$-phage DNA. (b) Height profile of the cross-section of the toroid at the position indicated by the bar in panel a. Notice that the toroid has a rather irregular structure with a cross-sectional diameter on the order of 75 nm and a height around 3 nm.

from the *B*- to the *A*-form. The double-stranded duplex in the *A*-form is thick with a diameter 2.6 nm and compressed in the longitudinal direction with a 3.2 nm pitch per turn of the helix. We were unable to determine the contour length of the condensed $\lambda$-phage DNA molecules after the rinse with ethanol. To obtain information about the DNA secondary structure, we measured the height of the protruding sections of the partially condensed toroidal structures (see Figure 2d). The average height of these sections was $1.6 \pm 0.4$ nm, which is, within experimental error, the same as the height of the individual DNA molecules as measured in the preparation procedure without rinsing with ethanol. We consider the similarity in the measured heights of the molecules as strong support that the brief rinsing with ethanol has not resulted in a change in the secondary structure of the duplex.

**Condensation Morphologies.** We further investigated the morphologies of the condensed DNA structures by analysis of the tapping mode AFM images. A close image of a typical toroid is displayed in Figure 3. The cross-section displayed in Figure 3b shows a void at the center of the condensed structure. This observation agrees with a toroid made of circumferentially wound DNA rather than a globular structure. The structure of the toroid is typically quite irregular; there are often protrusions or even gaps, and there is a strong variation in the lateral thickness and height along the contour of the toroid in the azimuthal direction. The distribution in azimuthally averaged inner diameter $D_i$, outer diameter $D_o$, height $H$, and lateral thickness $D_o - D_i$ in a population of 16 toroidal structures is shown in Figure 4. We obtained a rather broad distribution in these parameters. The inner diameter ranges from around 40 to 150 nm with a strong bias toward the smaller values. The toroids are fairly large with outer diameters in the range of 100−450 nm. As is often observed in surface-directed condensation, the toroids are disk-like with moderate heights as measured from the mica surface in the range 2.2−3.4 nm with a prevailing value of 2.8 nm.[5,6] In view of the fact that the duplex has an outer diameter of 2 nm, the toroids should hence be composed of one or two layers of DNA. The toroids are rather spread out with a lateral thickness between 50 and 200 nm, which corresponds to 20−70 concentric rings of DNA if the interaxial spacing between the duplexes is around 2.8 nm.

Individual toroids show an irregularity in both height and lateral dimensions in the azimuthal direction along the circular contour. For instance, the height of the toroid in Figure 3 ranges from 1.8 to 3.0 nm. Another illustrative example is the partially condensed toroid shown in Figure 2d. The extended part has a

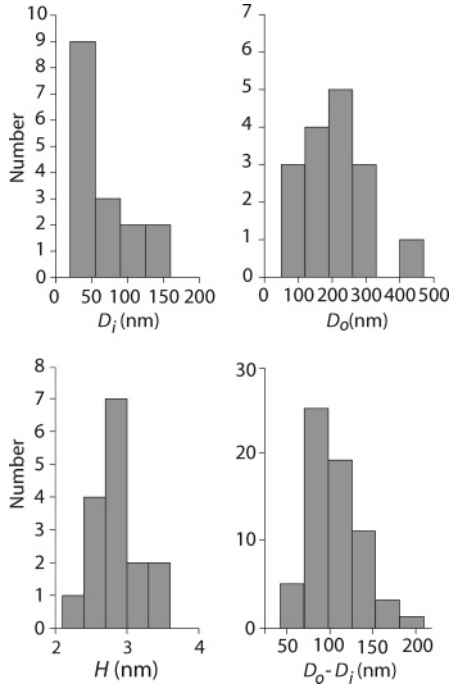


**Figure 4.** Distribution in inner diameter $D_i$, outer diameter $D_o$, height $H$, and lateral thickness $D_o - D_i$ in a population of 16 toroids.

height of $1.6 \pm 0.4$ nm, whereas the condensed part has a height in the range of 2−3 nm. For a subset of nine toroidal structures, we have listed the corresponding structural parameters in Table 1. Note that the standard deviations refer to the azimuthal variation along the contour of individual toroids rather than the statistics of the whole population of toroids. The variation in height is typically on the order of a nanometer. Similar to the variation in height, there is also a strong variation in the inner and outer diameters. As shown in Figure 5a, the standard deviation in the inner diameter increases with an increasing mean inner diameter and becomes on the order of 30% for the largest structures. The deviation from circular symmetry of a particular toroid also can be expressed as the ratio of the maximum and minimum values of the inner diameter. This aspect ratio versus the mean inner diameter is displayed in Figure 5b. From the results, it is clear that the smaller toroids with inner diameters in the range of 20−40 nm are fairly circular. With increasing size, however, the inner voids of the toroids become increasingly asymmetric with aspect ratios on the order of 3.

An important issue is as to whether the condensed structures are uni- or multi-molecular (i.e., do they contain a single or multiple $\lambda$-phage DNA molecules?). In principle, this question can be answered from an analysis of the volumes of the condensates. The determination of the volumes is, however, problematic because the toroids are very thin (one to two molecular layers) with a concomitant inaccuracy in height measurement due to surface effects (including roughness). A more accurate way to assess the composition is to analyze the spreading of the toroidal structure on the surface (i.e., its footprint). Let us consider a DNA molecule with contour length $L$ (16.5 $\mu$m for $\lambda$-DNA in the *B*-form) circumferentially wrapped in a toroidal structure with interhelix spacing $R$ and with inner and outer diameters $D_i$ and $D_o$, respectively. If the number of stacked layers is $n$ (as judged from the height, $n$ should be between one and two), the interaxial spacing follows from the total contour length stored in the toroid

$$\frac{R}{n} = \frac{\pi}{4L}(D_o^2 - D_i^2) \quad (1)$$

For the subset of nine toroids, the results are listed in Table 1. The interaxial spacing of bulk-phase condensed DNA structures is around 2.8 nm.[2,16] As judged from the entries in Table 1, the dimensions of toroid numbers 5 and 6 comply with one layer with an interaxial spacing of 2.7 nm ($n = 1$). Toroid numbers 1 and 2 are composed of two layers ($n = 2$), whereas toroid numbers 3 and 4 are intermediate, consisting of partially one and partially two layers. The inner and outer diameters hence comply with a single $\lambda$-phage DNA molecule circumferentially condensed in a toroidal structure spread out on the surface with tens of concentric rings of DNA and a height of one to two molecular layers.

In Table 1, toroid number 7 is exceptional in the sense that it has a very large inner and outer diameter and a large $R/n$ value. The latter value implies that the average spacing between the strands exceeds 7.3 nm (the minimum value of $n$ is obviously one). Another possibility is that the toroid accommodates multiple $\lambda$-phage DNA molecules. For instance, in the presence of two DNA molecules, the stored contour length doubles, and the minimum average interaxial spacing is reduced by a factor of 2 and takes the value of 3.6 nm. Close scrutiny of the corresponding AFM image in Figure 2c reveals that the toroid is, however, not closely packed and even exhibits some gaps in its structure. Accordingly, the large size and $R/n$ value do not necessarily imply that the toroid includes multiple $\lambda$-phage DNA molecules. The dimensions of exceptionally large toroids such as number 7 also can be rationalized in terms of the condensation of a single molecule but not closely packed with a relatively open morphology.

The $R/n$ values in Table 1 have been calculated with a contour length $L = 16.5$ $\mu$m pertaining to $\lambda$-phage DNA in the *B*-form. If the DNA molecules have undergone a transition from the *B*- to the *A*-form during the rinse with ethanol, their contour length decreased by 6% due to the concomitant change in helical pitch from 3.4 to 3.2 nm per turn of the helix. In this case, the values for $R/n$ in Table 1 are underestimated by 6%, but this has no effect on our conclusion regarding the single-molecular composition of the toroids.

Besides toroids, we also have observed rod-like condensed structures. The rod-like structures constitute no more than 10% of the total number of condensed structures and are therefore far less abundant. The lengths are in the range of 220−300 nm, widths in the range of 80−110 nm, and heights around 4 nm. The measured heights indicate that the rod-like structures contain two to three stacked DNA layers. On the basis of a single circumferentially wrapped DNA molecule, just as a toroidal structure with a collapsed void, the dimensions agree with an interaxial spacing in the range of 2.5−3 nm.

The variation in dimensions and the irregularity in condensed morphologies can be understood in terms of the pathway controlled ethanol-induced condensation process. During the rinse with ethanol, which is a poor solvent for DNA, the adsorbed DNA molecules minimize their interaction with the organic solvent by forming a nucleation loop followed by wrapping of the duplex around the nucleation loop in a circumferential manner. A similar mechanism has been proposed for condensation in the bulk phase,[2] but, here, the process is surface-directed because the DNA molecules remain adsorbed at the mica surface. For toroids, the size of the inner diameter

**TABLE 1: Inner Diameter $D_i$, Outer Diameter $D_o$, and Height $H$ of Some Toroidal Structures[a]**

| toroid number | 1 | 2 | 3 | 4 | 5 | 6 | 7 |
|---|---|---|---|---|---|---|---|
| $D_i$ (nm) | $42 \pm 4$ | $36 \pm 12$ | $56 \pm 16$ | $52 \pm 16$ | $58 \pm 20$ | $68 \pm 18$ | $95 \pm 37$ |
| $D_o$ (nm) | $162 \pm 14$ | $170 \pm 16$ | $214 \pm 18$ | $224 \pm 6$ | $246 \pm 14$ | $246 \pm 26$ | $404 \pm 19$ |
| $H$ (nm) | $2.7 \pm 0.7$ | $2.5 \pm 0.6$ | $3.1 \pm 0.4$ | $2.3 \pm 0.5$ | $3.4 \pm 0.6$ | $2.9 \pm 0.4$ | $3.5 \pm 0.3$ |
| $R/n$ | 1.2 | 1.3 | 2.0 | 2.3 | 2.7 | 2.7 | 7.3 |

[a] Standard deviations refer to the statistical average of measurements of a single toroidal structure in nine different directions away from the center of the toroid with an angular increment of 40°. Interaxial spacing divided by the number of layers $R/n$ was calculated according to eq 1 with a contour length $L = 16.5$ $\mu$m pertaining to $\lambda$-phage DNA in the *B*-form.

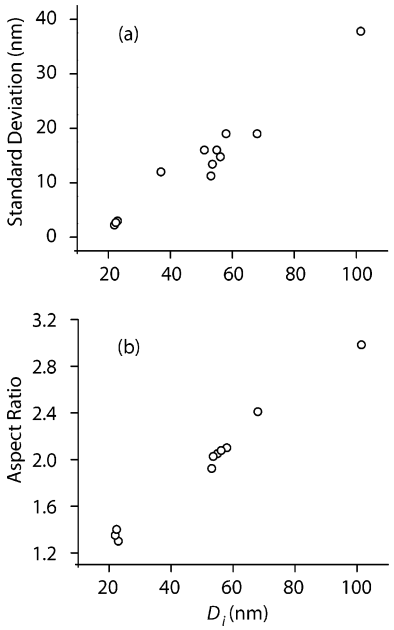


**Figure 5.** (a) Standard deviation in inner diameter vs the mean inner diameter measured in nine radial directions away from the center of the toroid with an increment in angle of 40°. (b) Ratio of the maximum and minimum inner diameter (aspect ratio) vs the mean inner diameter. Note that each data point refers to an individual toroidal structure.

is on the order of the bending persistence length of 50 nm, which complies with the bending energy of the nucleation loop on the order of the thermal energy $kT$. The competition between the unfavorable DNA−solvent interaction and the magnesium ion facilitated DNA−surface interaction eventually results in an overall thin disk-like structure. The toroidal structure is, however, not perfect; there is a strong variation in height and spread of the adsorbed DNA molecules due to the competing interactions.

The rod-like condensed structures may be formed by a similar mechanism. The condensation process is nucleated by the formation of a nucleation loop, but now the radius of curvature exceeds the bending persistence length and is on the order of 100−200 nm. As shown by the aspect ratios in Figure 5b, the inner voids of larger toroids are increasingly asymmetric, and opposing segments of the toroid may not be too far separated across the void. To reduce unfavorable DNA−ethanol interactions, but at the cost of extra bending energy at the end-points of the condensate, the larger nucleation loops and/or toroids are likely to collapse in a side-by-side manner and thereby form rod-like structures. Whether this happens at the nucleation stage or after the toroids already have been formed can unfortunately not be deduced from these imaging experiments.

## Conclusion

It is often, if not always, necessary to spot a highly diluted DNA solution on a surface to investigate the properties of single molecules in DNA adsorption studies. We have shown that the resulting DNA morphologies depend on the way the solutions are prepared. If the stock solution is diluted and if the specimens are developed in ultrapure, deionized water, flat-lying densely packed DNA networks are observed in agreement with earlier observations.[7,8] The height of the segments of the network, as measured with tapping mode AFM indicates that the DNA is single-stranded. Since the Watson−Crick double-helical structure of DNA is known to be unstable at minimal ionic strength under salt-free conditions, we suspect that the DNA double helix is (partially) melted in the sample preparation procedure. At the surface, the single DNA strands can hybridize with other strands pertaining to the same or other DNA molecules and thus form a network. This conjecture is supported by the fact that double-stranded, noncross-linked or hybridized DNA molecules are observed if the dilution and development procedures are carried out under TE buffer conditions so that the stability of the double helix is ensured.

The adsorbed single DNA molecules subsequently can be condensed in situ by a brief rinse of the specimens with anhydrous ethanol. It should be noted that the condensation occurs after adsorption of DNA onto the mica and that the process is assisted and directed by the surface. Furthermore, we obtained the condensed structures by a change in solvent quality in the presence of divalent magnesium (magnesium also serves to attach the DNA molecules to the surface). The predominant morphology is a toroid, but a small fraction of rod-like structures was also observed. Analysis of the height and lateral dimensions shows that the toroids are single-molecular and disk-like with a height of one to two DNA diameters. Thin toroidal structures previously have been observed in nucleoprotamine or cationic silane-induced DNA condensation studies on mica and silicon surfaces, respectively.[5,6] Accordingly, the thin toroid morphology appears to be a general phenomenon of surface-directed condensation, irrespective of the nature of the condensing ligands and the specific surface interaction. The rod-like structures may be formed by a side-by-side collapse of the inner (nucleation) loop of the larger toroidal structures. The condensed morphologies are not perfect. There is a strong variation in shape, height, and spread of the adsorbed DNA molecule, which can be attributed to the competing DNA−surface and solvent interactions in the pathway controlled condensation process.

## References and Notes

(1) Bloomfield, V. A. *Curr. Opin. Struct. Biol.* **1996**, *6*, 334−341.
(2) Hud, N. V.; Vilfan, I. D. *Annu. Rev. Biophys. Biomol. Struct.* **2005**, *34*, 295−318.
(3) Pelta, J.; Durand, D.; Doucet, J.; Livolant, F. *Biophys. J.* **1996**, *71*, 48−63.
(4) Raspaud, E.; Durand, D.; Livolant, F. *Biophys. J.* **2005**, *88*, 392−403.
(5) Allen, M. J.; Bradbury, E. M.; Balhorn, R. *Nucleic Acids Res.* **1997**, *25*, 2221−2226.
(6) Fang, Y.; Hoh, J. H. *Nucleic Acids Res.* **1998**, *26*, 588−593.
(7) Xiao, Z.; Xu, M.; Sagisaka, K.; Fujita, D. *Thin Solid Films* **2003**, *438−439*, 114−117.

(8) Song, Y.; Li, Z.; Liu, Z.; Wei, G.; Wang, L.; Sun, L.; Guo, C.; Sun, Y.; Yang, T. *J. Phys. Chem. B* **2006**, *110*, 10792−10798.

(9) Arscott, P. G.; Ma, C.; Wenner, J. R.; Bloomfield, V. A. *Biopolymers* **1995**, *36*, 345−364.

(10) Fang, Y.; Spisz, T. S.; Hoh, J. H. *Nucleic Acids Res.* **1999**, *27*, 1943−1949.

(11) Adamcika, J.; Klinovc, D. V.; Witza, G.; Sekatskiia, S. K.; Dietlera, G. *FEBS Lett.* **2006**, *580*, 5671−5675.

(12) Bustamante, C.; Vesenka, J.; Tang, C. L.; Rees, W.; Guthold, M.; Keller, R. *Biochemistry* **1992**, *31*, 22−26.

(13) Schaper, A.; Pietrasanta, L. I.; Jovin, T. M. *Nucleic Acids Res.* **1993**, *21*, 6004−6009.

(14) Thundat, T.; Allison, D. P.; Warmack, R. J. *Nucleic Acids Res.* **1994**, *22*, 4224−4228.

(15) Wilson, R. W.; Bloomfield, V. A. *Biochemistry* **1979**, *18*, 2192−2196.

(16) Schellman, J. A.; Parthasarathy, N. *J. Mol. Biol.* **1984**, *175*, 313−329.